Temperature thresholds of ecosystem respiration at a global scale.

Article

Accepted Version

Johnston, A. S. A. ORCID: https://orcid.org/0000-0001-8781-4039, Meade, A. ORCID: https://orcid.org/0000-0001-7095-7711, Ardö, J. ORCID: https://orcid.org/0000-0002-9318-0973, Arriga, N. ORCID: https://orcid.org/0000-0001-5321-3497, Black, A., Blanken, P. D. ORCID: https://orcid.org/0000-0002-7405-2220, Bonal, D. ORCID: https://orcid.org/0000-0001-9602-8603, Brümmer, C. ORCID: https://orcid.org/0000-0001-6621-5010, Cescatti, A., Dušek, J. ORCID: https://orcid.org/0000-0001-6119-0838, Graf, A. ORCID: https://orcid.org/0000-0003-4870-7622, Gioli, B. ORCID: https://orcid.org/0000-0001-7631-2623, Goded, I. ORCID: https://orcid.org/0000-0002-1912-325X, Gough, C. M. ORCID: https://orcid.org/0000-0002-1227-7731, Ikawa, H., Jassal, R. ORCID: https://orcid.org/0000-0002-6727-5215, Kobayashi, H. ORCID: https://orcid.org/0000-0001-9319-0621, Magliulo, V. ORCID: https://orcid.org/0000-0001-5505-6552, Manca, G. ORCID: https://orcid.org/0000-0002-9376-0310, Montagnani, L. ORCID: https://orcid.org/0000-0003-2957-9071, Moyano, F. E. ORCID: https://orcid.org/0000-0002-4090-5838, Olesen, J. E. ORCID: https://orcid.org/0000-0002-6639-1273, Sachs, T. ORCID: https://orcid.org/0000-0002-9959-4771, Shao, C., Tagesson, T. ORCID: https://orcid.org/0000-0003-3011-1775, Wohlfahrt, G. ORCID: https://orcid.org/0000-0003-3080-6702,

Temperature thresholds of ecosystem respiration at a global scale

Alice S.A. Johnston[1,2*], Andrew Meade[2], Jonas Ardö[3], Nicola Arriga[4], Andy Black[5], Peter D. Blanken[6], Damien Bonal[7], Christian Brümmer[8], Alessandro Cescatti[4], Jiří Dušek[9], Alexander Graf[10], Beniamino Gioli[11], Ignacio Goded[4], Christopher M. Gough[12], Hiroki Ikawa[13], Rachhpal Jassal[5], Hideki Kobayashi[14], Vincenzo Magliulo[15], Giovanni Manca[4], Leonardo Montagnani[16,17], Fernando E. Moyano[18], Jørgen E. Olesen[19], Torsten Sachs[20], Changliang Shao[21], Torbern Tagesson[22], Georg Wohlfahrt[23], Sebastian Wolf[24], William Woodgate[25,26], Andrej Varlagin[27], Chris Venditti[2]

[1] School of Water, Energy and Environment, Cranfield University, Bedfordshire, MK43 0AL, UK.
[2] School of Biological Sciences, University of Reading, Reading, RG6 6BX, UK.
[3] Physical Geography and Ecosystem Science, Lund University Sölvegatan 12, Sweden.
[4] European Commission, Joint Research Centre (JRC), Ispra, Italy.
[5] Faculty of Land and Food Systems; University of British Columbia; Vancouver, BC V6T 1Z4, Canada.
[6] Department of Geography, University of Colorado, Boulder CO, USA 80309-0260.
[7] Université de Lorraine, AgroParisTech, INRAE, UMR Silva, 54000 Nancy, France.
[8] Thünen Institute of Climate-Smart Agriculture, Bundesallee 65, 38116 Braunschweig, Germany.
[9] Global Change Research Institute of the Czech Academy of Sciences, CZ-60300 Brno, Czech Republic.
[10] Forschungszentrum Jülich, Institute for Bio- and Geosciences 3: Agrosphere, 52080 Jülich, Germany.
[11] CNR, Institute of Bioeconomy, 50145 Firenze, Italy.
[12] Virginia Commonwealth University, Department of Biology, Richmond, VA 23234, USA
[13] Institute for Agro-Environmental Sciences, National Agriculture and Food Research Organization, Tsukuba, 305-8604, Japan
[14] Research Institute for Global Change, Institute of Arctic Climate and Environment Research, Japan Agency for Marine-Earth Science and Technology, Japan.
[15] CNR, Institute for Mediterranean Agriculture and Forest Systems, 85 80040 Ercolano, Italy.
[16] Autonomous Province of Bolzano, Forest Services, Bolzano 39100, Italy.
[17] Faculty of Science and Technology, Free University of Bolzano, Bolzano 39100, Italy
[18] University of Goettingen, Bioclimatology, Büsgenweg 2, 37077 Göttingen, Germany
[19] Aarhus University, Department of Agroecology, Blichers Allé 20, 8830 Tjele, Denmark
[20] GFZ German Research Centre for Geoscience, Telegrafenberg, Potsdam, Germany
[21] Institute of Agricultural Resources and Regional Planning, Chinese Academy of Agricultural Sciences, Beijing 100081, China.
[22] Department of Geosciences and Natural Resources, University of Copenhagen, Öster Voldgade 10, Copenhagen, Denmark.
[23] Department of Ecology, University of Innsbruck, 6020 Innsbruck, Austria.
[24] Department of Environmental Systems Science, ETH Zurich, 8092 Zurich, Switzerland.
[25] Land & Water, Commonwealth Scientific and Industrial Research Organisation, 2601, Canberra, Australia
[26] School of Earth and Environmental Sciences, The University of Queensland, 4067, Queensland, Australia.
[27] A.N. Severtsov Institute of Ecology and Evolution, Russian Academy of Sciences, 119071, Leninsky pr.33, Moscow, Russia
*Correspondence: a.s.johnston@cranfield.ac.uk

Abstract

Ecosystem respiration is a major component of the global terrestrial carbon cycle and is strongly influenced by temperature. The global extent of the temperature-ecosystem respiration relationship, however, has not been fully explored. Here, we test linear and threshold models of ecosystem respiration across 210 globally distributed eddy covariance sites covering the most extensive temperature range ever studied. We find thresholds to the global temperature-ecosystem respiration relationship at high and low air temperatures and mid soil temperatures, which represent transitions in the temperature dependence and sensitivity of ecosystem respiration. Annual ecosystem respiration rates show a markedly reduced temperature dependence and sensitivity compared to half-hourly rates, and a single mid-temperature threshold for both air and soil temperature. Our study indicates a distinction in the influence of environmental factors, including temperature, on ecosystem respiration between latitudinal and climate gradients at short (half-hourly) and long (annual) timescales. Such climatological differences in the temperature sensitivity of ecosystem respiration have important consequences for the terrestrial net carbon sink under ongoing climate change.

Main

Carbon losses from terrestrial ecosystems determine the direction and magnitude of carbon-climate feedbacks[1,2]. The trajectory of future climate change therefore depends on the biological processes that underpin ecosystem fluxes. Ecosystem respiration (R_e), the cumulative respiration of autotrophs (plants) and heterotrophs (bacteria, fungi and animals), represents a major component of the global carbon cycle[3]. Temperature strongly influences R_e through the laws of thermodynamics[4–6], but the global extent of the temperature-R_e relationship has not been fully explored[7,8].

Temperature-mediated variations in R_e are typically described as an exponential function in Earth system models (ESMs)[2]. That is, globally static Q_{10} values of around 2 represent a doubling of ecosystem CO_2 fluxes with an increase in temperature of 10 °C, when all other terms are equal[9]. Empirical and theoretical studies, however, have documented conflicting temperature-R_e relationships. Latitudinal shifts in the temperature sensitivity of R_e have been observed in empirical studies, with ecosystems experiencing greater increases in R_e with temperature at high, compared to mid and low, latitudes[8,10,11]. At the same time, global syntheses have proposed convergent temperature sensitivities of R_e across different climates and ecosystem types[4,12,13].

The influence of temperature on ecosystem respiration is mediated by the temperature sensitivity of individual physiology, community composition and biotic interactions of all the organisms inhabiting an ecosystem[13,14]. At the individual-level, metabolic rates scale with

body mass and increase exponentially with temperature according to the Boltzmann factor, $e^{-E/kT}$, where E is the activation energy (eV), k is the Boltzmann's constant (8.62×10^{-5} eV K^{-1}), and T is temperature (in Kelvin)[6]. Widescale application of the Boltzmann factor to individual metabolic rates has revealed a common value of E between 0.6 and 0.7 eV[5,6,15]. At the ecosystem-level, models based on metabolic theory indicate exponential temperature-R_e relationships across diverse ecosystems with a value of E surprisingly similar to individual metabolic rates (0.65 eV; Q_{10} ~ 2.50[4,13]). Yet, models of the temperature-R_e relationship have focused on a limited temperature range between 0 and 30 °C, even though terrestrial ecosystems experience temperatures between -60 and 50 °C[16].

In this study we test the generality of the temperature-R_e relationship, described by a general ecosystem model, across the most extensive temperature range yet investigated. The model, founded in metabolic theory, gives the linear expression:

$$\ln(R_e) = \frac{-E}{1{,}000k}\left(\frac{1{,}000}{T}\right) + \ln[(b_0)(C)] \quad (1)$$

where $\ln(R_e)$ is the natural logarithm of ecosystem respiration, in W ha^{-1}; (1,000/T) is the reciprocal of absolute temperature; b_0 is the intensity of cellular metabolism; and C is the size distribution of organisms (assumed to be independent of R_e according to the energy equivalence rule)[4]. The model predicts a general linear relationship between (1,000/T) and $\ln(R_e)$, with an expected slope ($\bar{E}$ from hereon in) across diverse ecosystems equal to -7.50 K (0.65 eV, with a plausible range between -2 and -11 K, or 0.2 and 1.2 eV)[10]. However, we would expect climatological differences in resource supply[17,18] and community composition[14,19] to alter $\bar{E}$ across the global temperature range. We would also expect divergent relationships between metabolism and resource supply with temperature to modify the temperature-R_e relationship over time[13,20].

Results

We test the global extent of the linear temperature-R_e relationship predicted by metabolic theory, by applying the model presented in Eq. 1 to measurements across 210 globally distributed FLUXNET sites[21] (Figure 1 and Supplementary Data 1). Both short-term (half-hourly) and long-term (annual) measurements were tested for air and soil temperature. The half-hourly FLUXNET dataset is presented with more conventional temperature and R_e units in Extended Data 1. The linear model (Eq. 1) was compared to a threshold model, which accounts for variations in the activation energy ($\bar{E}$) in Eq. 1 above and below specified temperature breakpoints (see Methods). That is, the threshold model accounts for shifts in the temperature sensitivity of R_e across the global temperature range, and explains latitudinal shifts in the temperature-R_e relationship observed in empirical studies[8,10,11]. All

models were linear mixed effects models and goodness of fit comparisons used Akaike Information Criterion (AIC) measurements.

Figure 1

The threshold model, which integrated two temperature breakpoints of -24.8 ±0.15 and 15.1 ±0.22 °C, better explained R_e rates over the global extent of air temperatures in the FLUXNET dataset than the linear model (ΔAIC = 3,839,265, Figure 2). Similar to previous findings[4,13], the threshold model indicates a temperature sensitivity of R_e indistinguishable from that of -7.50 K (0.65 eV, dashed line in Figs. 2a & b) predicted by metabolic theory (likelihood ratio test: $\chi^2 = 0$, $p = 1$) between temperature breakpoints ($\bar{E}$ = -7.42 K, 0.64 eV, Q_{10} ~ 2.45 between 15.1 and -24.8 °C, solid line in Fig. 2b). Evaluation of the linear model, on the other hand, gives an activation energy for global R_e rates of -7.30 K (0.63 eV, solid lines in Fig. 2a), significantly different from that predicted by metabolic theory (likelihood ratio test: $\chi^2 = 20009$, $p < 0.0001$). Importantly, the threshold model indicates a lower temperature sensitivity of R_e at higher temperatures ($\bar{E}$ = -2.84 K, 0.25 eV, Q_{10} ~ 1.41 above 15.1 °C) and extreme temperature sensitivity of R_e at very low temperatures ($\bar{E}$ = -30.53 K, 2.64 eV, Q_{10} ~ 40.79 below -24.8 °C). The threshold model therefore primarily improves predictions, compared to the linear model, of the temperature-R_e relationship at low and high latitude sites (Figs. 2f & g). High measured variability in R_e across the global temperature range, however, likely reflects the interactive effects of disturbance events, plant phenology and soil water and nutrient limitation on ecosystem metabolism.

Figure 2

Given the importance of belowground communities in R_e[14,19], linear and threshold models were tested for the global relationship between soil temperature and ecosystem respiration (Figure 2 and Supplementary Table 2). A single temperature threshold of 11.4 ±0.29 °C emerged for soil temperature, with little evidence for a lower temperature breakpoint (likelihood ratio test: $\chi^2 = 0$, $p = 1$). Above the temperature threshold, the activation energy of R_e was lower than that observed for air temperature ($\bar{E}$ = -2.18 K, 0.19 eV, Q_{10} ~ 1.30), while below the temperature threshold the activation energy was steeper than that between air temperature thresholds ($\bar{E}$ = -13.37 K, 1.16 eV, Q_{10} ~ 5.05). The absence of a lower threshold for R_e with soil temperature is likely explained by thermal insulation from snow cover at low temperatures[22] resulting in much fewer observations, compared to air temperature, of the soil temperature-R_e relationship below 0 °C.

To account for the relative uncertainties of eddy covariance measurements below -20 °C[23], alongside the emergence of a single temperature breakpoint for soil temperature, we tested the sensitivity of the air temperature threshold model to temperature ranges with few

146 available measurements (Extended Data 2). Ecosystem respiration data were classified in 5
147 °C temperature intervals and intervals containing < 1% of all measurements (n < 235,521)
148 were defined as low frequency intervals. Such intervals were present at both high (> 36 °C)
149 and low (< -19 °C) temperatures. Each low frequency temperature interval was removed one
150 by one, as well as all together (~ 1.8 % of the dataset), to investigate the sensitivity of the
151 threshold model. The test provides supporting evidence of the robustness of temperature
152 breakpoints to the removal of each temperature interval one by one. However, there was no
153 support for a lower temperature breakpoint (-24.8 °C in Fig. 2b & c) when all low frequency
154 intervals or all those < -19 °C were removed. Instead, a single temperature breakpoint of
155 14.6 °C emerged (Extended Data 3 and Supplementary Table 3). The lower air temperature
156 breakpoint should therefore be considered with caution until more accurate R_e
157 measurements at low temperatures can be made. R_e rates nevertheless display a sharp
158 decline at lower temperatures for both air (Fig. 2b) and soil (Fig. 3b) temperatures.

159 **Figure 3**

160 Sharp declines in R_e at low soil and air temperatures likely indicate pulse responses of soil
161 respiration to rewetting and thawing events[24], attributed to the suppression of microbial
162 activity under water limitation in freezing conditions[25] and an uncoupling of the temperature
163 dependence of microbial respiration from thermodynamic laws[26]. Differences between global
164 temperature-R_e relationships for air and soil temperature at short timescales also suggest
165 shifts in the contribution of aboveground and belowground communities to R_e across the
166 global extent of temperatures. For instance, a lower activation energy for the temperature-R_e
167 relationship at higher soil temperatures ($\bar{E}$ = -2.18 K > 11.4 ±0.29 °C, Fig. 3), compared to air
168 temperatures ($\bar{E}$ = -2.84 K > 15.1 °C, Fig. 2), could indicate a relative reduction in the
169 contribution of belowground autotrophs and heterotrophs to R_e in warmer climates. On the
170 other hand, the lower threshold for the temperature-R_e relationship at low air temperatures
171 could reflect a temperature limit for the metabolism of aboveground communities, whereas
172 the absence of a lower temperature threshold for soil temperature suggests the importance
173 of belowground communities as components of R_e in mild to cold climates.

174 Global air temperature thresholds were consistent across climates, but the goodness of fit of
175 the threshold model (pseudo r^2 and ΔAICs compared to the linear model, Fig. 4) declined
176 with a decrease in overall temperature range at lower latitudes. For instance, the
177 temperature dependence of R_e (variation in R_e rates explained by temperature) was greater
178 in cold, higher latitude, climates (tundra and boreal, r^2_m > 0.60), compared to mild
179 (temperate, r^2_m = 0.48) and warm, low latitude, climates (mediterranean and tropical, r^2_m ≤
180 0.09). In warmer climates, random effects had a much greater influence on R_e than in mild or
181 cold climates, with FLUXNET site and latitude explaining more variation in tropical and

mediterranean ecosystems (Supplementary Table 4). Across the 210 sites, the threshold model better predicted the temperature-R_e relationship in the majority of cases (n = 197, Supplementary Data 1), while temperature explained more of the variation in R_e rates at sites with greater temperature ranges and higher latitudes (and Extended Data 4).

Q_{10} estimates from the threshold model reflect latitudinal shifts in the temperature sensitivity of ecosystem respiration, with tropical, mediterranean, temperate, boreal, and tundra climates yielding Q_{10} values of 1.38 ±0.01, 1.82 ±0.43, 2.32 ±0.31, 2.67 ±0.10, and 2.90 ±0.12 respectively, compared to a global Q_{10} of 2.26 ±0.35, and higher Q_{10} estimates based on the soil temperature threshold model (Supplementary Table 5). Empirical observations of R_e, soil respiration and carbon turnover rates are comparable with threshold model estimates of higher temperature sensitivities of R_e at high-latitudes and lower temperature sensitivities of R_e at low-latitudes[10,27]. Weaker temperature control in the linear model, similar to ESMs that implement static global Q_{10} values, cannot capture shifts in R_e temperature sensitivities across the global temperature range (Supplementary Table 5).

Figure 4

Annual temperature-R_e relationships were analysed across site years to investigate whether climatological differences in the temperature dependence and sensitivity of R_e emerge over longer timescales. The threshold model explained the temperature-R_e relationship better than the linear model at longer timescales for both air and soil temperature (Fig. 5). Surprisingly, threshold models converged for air and soil temperature, with a single mid-temperature breakpoint of 11.0 ±0.16 °C (Figs 5b & d). Above the temperature threshold, annual R_e rates declined with increasing mean annual temperatures from mid to low latitudes, while the activation energy below the temperature threshold was markedly reduced (Figs 5a & c, $\bar{E}$ ~ -4.90 K, 0.42 eV) compared to short timescales. Weaker temperature relationships at longer timescales is reflected by global Q_{10} estimates of 1.34 ±0.55 and 1.29 ±0.58 for air and soil temperature, respectively (Supplementary Table 6). An overall lack of R_e variation explained by temperature (r^2_m < 0.14) likely reflects the importance of confounding effects from soil water, nutrient limitation, and resource availability, alongside thermal acclimation, at longer timescales. The threshold model was further consistent for annual soil respiration and air temperature measurements from the Global Soil Respiration Database[28], with a single temperature breakpoint of 5.5 °C (Extended Data 5 and Supplementary Table 6).

Figure 5

Discussion

Our study shows how latitudinal shifts in R_e temperature sensitivity at both short and long timescales correspond to transitions in the global temperature–R_e relationship across temperature thresholds. Importantly, temperature thresholds also indicate differences in the temperature dependence of R_e, with more variation in R_e rates explained by temperature in cold compared to warm climates. In cold climates, temperature strongly influences metabolic activity of belowground microbial communities[19,25,26]. In warm climates, ecosystem metabolism is limited by water and nutrient availability, and resource availability to biological communities[18,27,29–31].

Both the temperature sensitivity and dependence of annual R_e rates is markedly reduced compared to the short-term R_e temperature response, suggesting the dominance of resource effects on ecosystem metabolism at longer timescales[13]. For instance, primary production directs carbon availability for ecosystem metabolism and typically shows a weaker temperature dependence[20,32]. Nutrient availability further drives preferential allocation of photosynthate C above- or below-ground, with consequences for carbon availability and quality to different ecosystem components[17].

Thresholds to the temperature-R_e relationship shown here will undoubtedly result from temporally divergent sensitivities between ecosystem components (e.g. below- and above-ground, heterotrophic and autotrophic) and several environmental controls over time. Variable acclimation of the different components of R_e to these environmental controls may further influence the temperature dependence and sensitivity of R_e by modifying the temperature response of catabolic and anabolic pathways[33–35]. Although we would expect such mechanisms to occur as gradual state changes rather than the sharp breakpoints described here, our study indicates consistent temperature thresholds at which ecosystem metabolism changes at a global scale. However, such results need to be validated for different ecosystem components as detailed measurements become available, and for decadal timescales over which the influence of anthropogenic factors can be detected.

Biosphere feedbacks with future climate changes will be strongly influenced by the temperature-R_e relationship[36,37] and latitudinal shifts in R_e temperature sensitivity as identified here will have important consequences for the global net land carbon sink[38]. For instance, while huge stores of labile carbon in permafrost regions could be released if temperatures rise above lower thresholds for microbial decomposition[26], CO_2 fertilisation in tropical and boreal regions could enhance carbon gains through primary production relative to losses through R_e[30,39]. Climate change forecasts by ESMs would thus be improved by accounting for temperature thresholds of R_e at a global scale. A higher resolution

understanding of R_e-climate feedbacks, however, requires strategic disentangling of the multiple environmental controls on the aboveground, belowground, heterotrophic, and autotrophic components of terrestrial ecosystem carbon fluxes.

Methods

The FLUXNET dataset

FLUXNET is a global network of micrometeorological sites providing eddy covariance CO_2 exchange observations between terrestrial ecosystems and the atmosphere[21]. The FLUXNET 2015 dataset used in this study provides half hourly temperature and night-time R_e measurements over 1454 site years and a latitudinal range of 78.92 °N to 37.43 °S. Observations across the 210 sites, which range from arctic tundra to tropical rainforest ecosystems, provide an extensive temperature range of 89.7 °C, from -43.4 to 46.3 °C (Figure 1 and Supplementary Data 1).

The FLUXNET dataset is subject to a data processing pipeline which include data quality controls checks, filtering of low turbulence periods and partitioning of CO_2 fluxes into respiration and photosynthesis components using established methods[21]. Disentangling respiration and photosynthesis fluxes during the day is complex and the extraction of R_e relies on modelling techniques with high uncertainty. Night-time CO_2 exchange measurements thus provide the best approximation of R_e, and uncertainty has been minimised for the FLUXNET dataset by employing quality control procedures[21]. Here, non-gap-filled half hourly (μmol CO_2 m^{-2} s^{-1}) and annual (g C m^{-2}) night-time R_e (RECO_NT_VUT_MEAN), air temperature (TA_F) and soil temperature (TS_F) measurements were compiled from the FLUXNET 2015 dataset (https://fluxnet.fluxdata.org/data/fluxnet2015-dataset/). R_e measurements were then converted to units of metabolic energy (W ha^{-1})[4] by taking 0.272 J μmol CO_2 and 10,000 m^2 ha^{-1}.

Model analysis

The linear model (1) for describing the temperature-R_e relationship was fitted to the global FLUXNET dataset, for both air and soil temperature. To test for the presence of temperature thresholds to the linear temperature–R_e model at a global scale, which explain shifts in R_e temperature sensitivity across climates, we compare the linear model in Eq. 1 to a threshold (piecewise) model. The threshold model, with two temperature breakpoints, gives:

$$\ln(Re) = \bar{E}_1 f_1(1{,}000/T, k_1) + \bar{E}_2 f_2(1{,}000/T, k_1, k_2)\, k2) + \bar{E}_3 f_3(1{,}000/T, k_2) + \ln[(b_0)(C)] \quad (2)$$

where $\bar{E}_1$, $\bar{E}_2$ and $\bar{E}_3$ represent activation energies for different temperature (1,000/T) ranges, determined by the two temperature breakpoints (k_1 and k_2) and f represents the functions:

$$f_1 = \begin{cases} 1{,}000/T, & 1{,}000/T \le k_1 \\ k_1, & k_1 > 1{,}000/T \end{cases}$$

$$f_2 = \begin{cases} 0, & 1{,}000/T \le k_1 \\ 1{,}000/T - k_1, & k_1 \le 1{,}000/T \le k_2 \\ k_2 - k_1, & 1{,}000/T > k_2 \end{cases}$$

$$f_3 = \begin{cases} 0, & 1{,}000/T \le k_2 \\ 1{,}000/T, & 1{,}000/T > k_2 \end{cases}$$

The threshold model first introduced a single temperature breakpoint to the linear model, so that the activation energy ($\bar{E}$, with more negative values indicating higher temperature sensitivity) varies above and below a specified temperature. Temperature breakpoints were tested for the temperature (1,000/*T*) range between 3.1 and 4.4, for every increment of 0.001 (~0.07 °C). Differences in linear and threshold model AIC's were then compared for every temperature breakpoint. The highest ΔAIC was taken as providing the most support for a temperature breakpoint, as long as ΔAIC > 5 for additional degrees of freedom and $p < 0.05$ in a likelihood ratio test. Then, the threshold model integrated an additional temperature breakpoint, taking the first temperature breakpoint with the greatest support as a fixed value. Model AIC's for each second temperature breakpoint were compared to the single threshold model and the second threshold was selected based on the highest ΔAIC given the conditions outlined above. Temperature breakpoints were identified for short (half-hourly) and long (annual) temperature-R_e relationships.

All models were linear mixed effects models, with FLUXNET site and latitude set as random effects. First, the models were tested for the global dataset and then for broadly classified climate zones (cold, mild, and warm) and climates (tundra, boreal, temperate, mediterranean, and tropical). Some generalisations were necessary during climate classification. For instance, alpine sites at mid-latitudes were classified as boreal climates (Supplementary Data 1). Linear and threshold models were further tested for each FLUXNET site. Finally, annual R_e rates were used to investigate changes in temperature breakpoints, and linear and threshold model performance, at long timescales for air and soil temperature. Long timescale models accounted for latitude and year as random effects.

References

1. Cao, M. & Woodward, F. I. Dynamic responses of terrestrial ecosystem carbon cycling to global climate change. *Nature* **393**, 249–252 (1998).

2. Heimann, M. & Reichstein, M. Terrestrial ecosystem carbon dynamics and climate feedbacks. *Nature* **451**, 289–292 (2008).
3. Allen, A. P., Gillooly, J. F. & Brown, J. H. Linking the global carbon cycle to individual metabolism. *Funct. Ecol.* **19**, 202–213 (2005).
4. Enquist, B. J. *et al.* Scaling metabolism from organisms to ecosystems. *Nature* **423**, 639–642 (2003).
5. Gillooly, J. F., Brown, J. H., West, G. B., Savage, V. M. & Charnov, E. L. Effects of size and temperature on metabolic rate. *Science* **293**, 2248–2251 (2001).
6. Brown, J. H., Gillooly, J. F., Allen, A. P., Savage, V. M. & West, G. B. Toward a metabolic theory of ecology. *Ecology* **85**, 1771–1789 (2004).
7. Friedlingstein, P. *et al.* Uncertainties in CMIP5 climate projections due to carbon cycle feedbacks. *J. Clim.* **27**, 511–526 (2014).
8. Davidson, E. A. & Janssens, I. A. Temperature sensitivity of soil carbon decomposition and feedbacks to climate change. *Nature* **440**, 165–173 (2006).
9. Lenton, T., M. & Huntingford, C. Global terrestrial carbon storage and uncertainties in its temperature sensitivity examined with a simple model. *Glob. Change Biol.* **9**, 1333–1352 (2003).
10. Song, B. *et al.* Divergent apparent temperature sensitivity of terrestrial ecosystem respiration. *J. Plant Ecol.* **7**, 419–428 (2014).
11. Lloyd, J. & Taylor, J. A. On the temperature dependence of soil respiration. *Funct. Ecol.* 315–323 (1994).
12. Mahecha, M. D. *et al.* Global Convergence in the Temperature Sensitivity of Respiration at Ecosystem Level. *Science* **329**, 838–840 (2010).
13. Yvon-Durocher, G. *et al.* Reconciling the temperature dependence of respiration across timescales and ecosystem types. *Nature* **487**, 472–476 (2012).
14. Johnston, A. S. A. & Sibly, R. M. The influence of soil communities on the temperature sensitivity of soil respiration. *Nat. Ecol. Evol.* **2**, 1597–1602 (2018).

15. Dell, A. I., Pawar, S. & Savage, V. M. Systematic variation in the temperature dependence of physiological and ecological traits. *Proc. Natl. Acad. Sci.* **108**, 10591–10596 (2011).
16. Buckley, L. B. & Huey, R. B. Temperature extremes: geographic patterns, recent changes, and implications for organismal vulnerabilities. *Glob. Change Biol.* **22**, 3829–3842 (2016).
17. Gill, A. L. & Finzi, A. C. Belowground carbon flux links biogeochemical cycles and resource-use efficiency at the global scale. *Ecol. Lett.* **19**, 1419–1428 (2016).
18. Green, J. K. *et al.* Large influence of soil moisture on long-term terrestrial carbon uptake. *Nature* **565**, 476–479 (2019).
19. Allison, S. D., Wallenstein, M. D. & Bradford, M. A. Soil-carbon response to warming dependent on microbial physiology. *Nat. Geosci.* **3**, 336–340 (2010).
20. Michaletz, S. T., Cheng, D., Kerkhoff, A. J. & Enquist, B. J. Convergence of terrestrial plant production across global climate gradients. *Nature* **512**, 39–43 (2014).
21. Pastorello, G. *et al.* The FLUXNET2015 dataset and the ONEFlux processing pipeline for eddy covariance data. *Sci. Data* **7**, 225 (2020).
22. Monson, R. K. *et al.* Winter forest soil respiration controlled by climate and microbial community composition. *Nature* **439**, 711–714 (2006).
23. Mauder, M. *et al.* A strategy for quality and uncertainty assessment of long-term eddy-covariance measurements. *Agric. For. Meteorol.* **169**, 122–135 (2013).
24. Kim, D.-G., Vargas, R., Bond-Lamberty, B. & Turetsky, M. R. Effects of soil rewetting and thawing on soil gas fluxes: a review of current literature and suggestions for future research. *Biogeosciences* **9**, 2459–2483 (2012).
25. Du, E. *et al.* Winter soil respiration during soil-freezing process in a boreal forest in Northeast China. *J. Plant Ecol.* **6**, 349–357 (2013).
26. Schuur, E. A. *et al.* Climate change and the permafrost carbon feedback. *Nature* **520**, 171–179 (2015).

27. Koven, C. D., Hugelius, G., Lawrence, D. M. & Wieder, W. R. Higher climatological temperature sensitivity of soil carbon in cold than warm climates. *Nat. Clim. Change* **7**, 817–822 (2017).
28. Bond-Lamberty, B. P. & Thomson, A. M. A Global Database of Soil Respiration Data, Version 4.0. *ORNL DAAC* (2018) doi:https://doi.org/10.3334/ORNLDAAC/1578.
29. Zhang, Z. *et al.* A temperature threshold to identify the driving climate forces of the respiratory process in terrestrial ecosystems. *Eur. J. Soil Biol.* **89**, 1–8 (2018).
30. Yang, Y., Donohue, R. J., McVicar, T. R., Roderick, M. L. & Beck, H. E. Long-term CO2 fertilization increases vegetation productivity and has little effect on hydrological partitioning in tropical rainforests. *J. Geophys. Res. Biogeosciences* **121**, 2125–2140 (2016).
31. Fleischer, K. *et al.* Amazon forest response to CO 2 fertilization dependent on plant phosphorus acquisition. *Nat. Geosci.* **12**, 736–741 (2019).
32. Padfield, D. *et al.* Metabolic compensation constrains the temperature dependence of gross primary production. *Ecol. Lett.* **20**, 1250–1260 (2017).
33. Atkin, O. K. & Tjoelker, M. G. Thermal acclimation and the dynamic response of plant respiration to temperature. *Trends Plant Sci.* **8**, 343–351 (2003).
34. Huntingford, C. *et al.* Implications of improved representations of plant respiration in a changing climate. *Nat. Commun.* **8**, 1602 (2017).
35. Niu, S. *et al.* Thermal optimality of net ecosystem exchange of carbon dioxide and underlying mechanisms. *New Phytol.* **194**, 775–783 (2012).
36. Rind, D. The Consequences of Not Knowing Low- and High-Latitude Climate Sensitivity. *Bull. Am. Meteorol. Soc.* **89**, 855–864 (2008).
37. Liu, Z. *et al.* Increased high-latitude photosynthetic carbon gain offset by respiration carbon loss during an anomalous warm winter to spring transition. *Glob. Change Biol.* **26**, 682–696 (2020).
38. Haverd, V. *et al.* Higher than expected CO2 fertilization inferred from leaf to global observations. *Glob. Change Biol.* **26**, 2390–2402 (2020).

396 39. Tagesson, T. *et al.* Recent divergence in the contributions of tropical and boreal forests
397 to the terrestrial carbon sink. *Nat. Ecol. Evol.* **4**, 202–209 (2020).

398

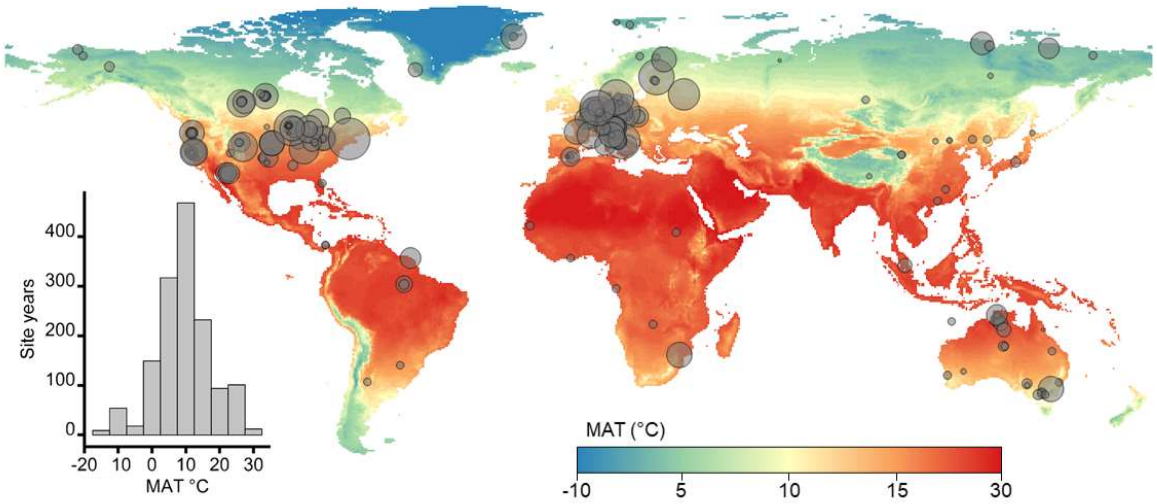

399

400 **Figure 1. Global distribution of the FLUXNET sites.** Site locations (n = 210) are displayed over a
401 world mean annual temperature (MAT) map. Symbol diameter represents the number of site years
402 (range: 1 to 22 years) and the inset left-hand figure shows the distribution of site years (n = 1454) by
403 MAT.

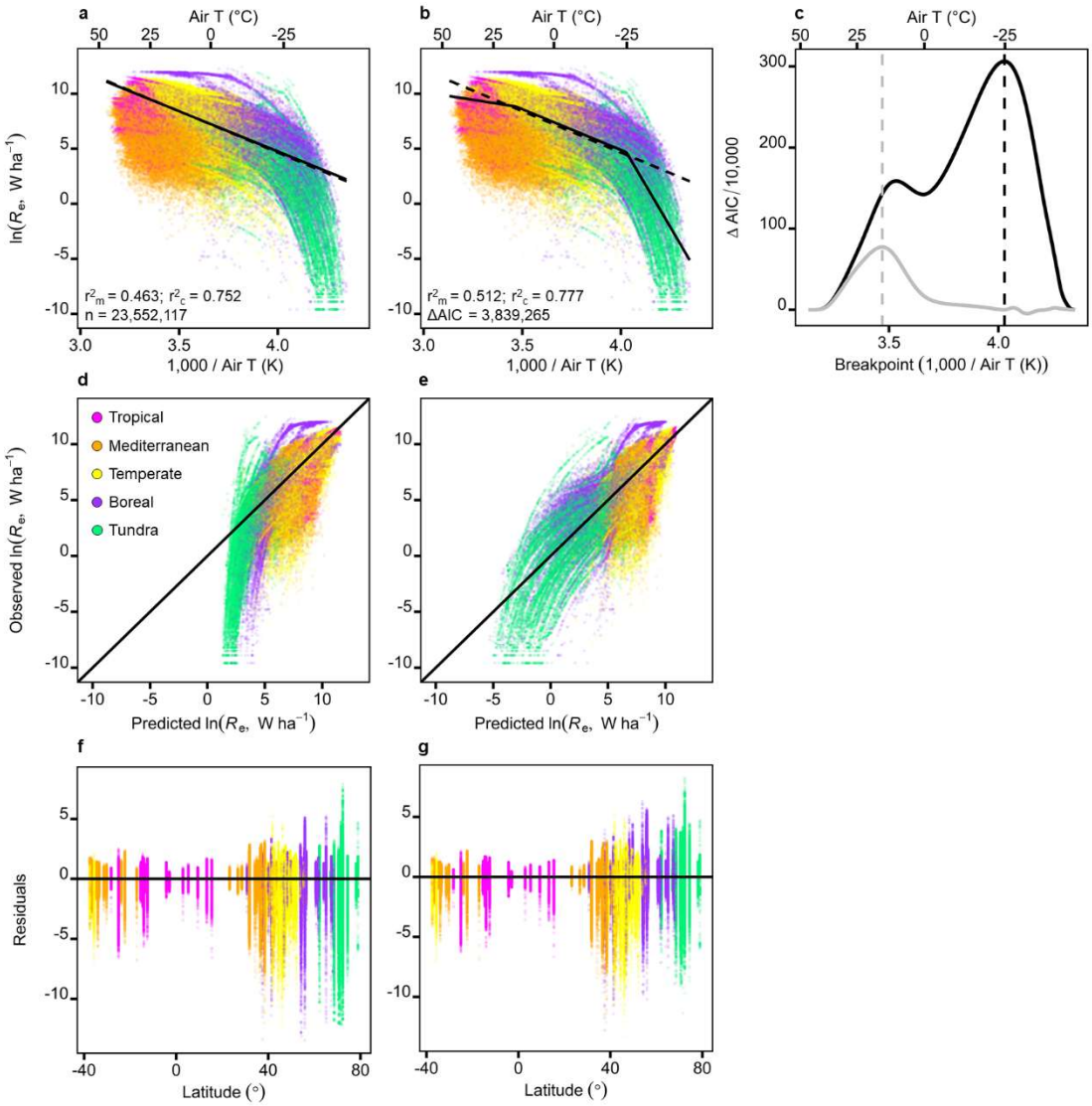

Figure 2. Global extent of the temperature-ecosystem respiration (R_e) relationship. Night-time half hourly ecosystem respiration measurements from the FLUXNET dataset (symbols), broadly classified as tropical (magenta), mediterranean (orange), temperate (yellow), boreal (purple) or tundra (green) climates. Left-hand plots (a, d & f) present predictions from the linear model (Eq. 1) and middle plots (b,e & g) from a threshold model with two temperature breakpoints (Eq. 2), of the temperature-ecosystem respiration relationship. The right-hand plot (c) shows the presence of two temperature breakpoints (black line: air (1,000/T)= 4.027, -24.8 °C; grey line: air (1,000/T) = 3.469, 15.1 °C), identified by the threshold models performance (ΔAIC's compared to the linear model where higher values provide a better fit to the FLUXNET dataset). Goodness of fit measures indicate the pseudo r^2 for marginal (fixed) effects (r^2_m) and conditional (fixed and random) effects (r^2_c), with top plots (a & b) showing predictions of the fixed effects only (temperature, solid lines) in each model compared to the activation energy of -7.50 K predicted by metabolic theory (dashed lines, r^2_m = 0.361; r^2_c = 0.542). Middle plots (d & e) present model predictions against observed FLUXNET measurements (solid black 1:1 lines would demonstrate perfect prediction), and bottom plots (f & g) show model residuals against latitude. Full details of the linear mixed effects models are presented in Supplementary Table 1.

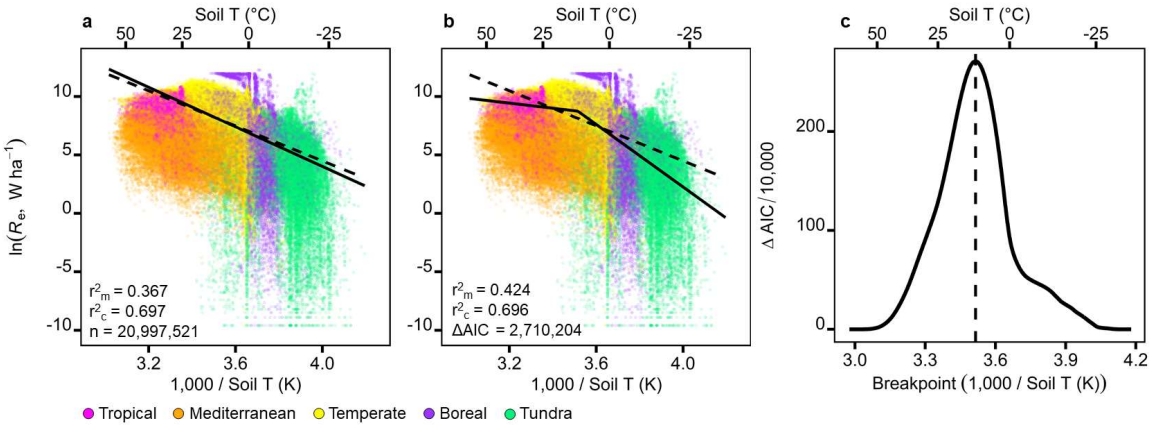

Figure 3. The global soil temperature-ecosystem respiration relationship. Night-time half hourly ecosystem respiration measurements from the FLUXNET dataset (symbols), broadly classified by climate with symbol colours as in Figure 2. Predictions of the temperature-ecosystem respiration relationship are compared for a) the linear model and b) the threshold model, for the fixed effects of temperature (solid lines). Both models are compared to the activation energy of -7.50 K predicted by metabolic theory (dashed lines, $r^2_m = 0.173$, $r^2_c = 0.500$). The right-hand plot (c) shows the presence of a single temperature breakpoints (black line: soil (1,000/*T*) = 3.515, 11.4 °C), identified by the threshold models performance (ΔAIC's compared to the linear model where higher values provide a better fit to the FLUXNET dataset). Full details of the linear mixed effects models are presented in Supplementary Table 2.

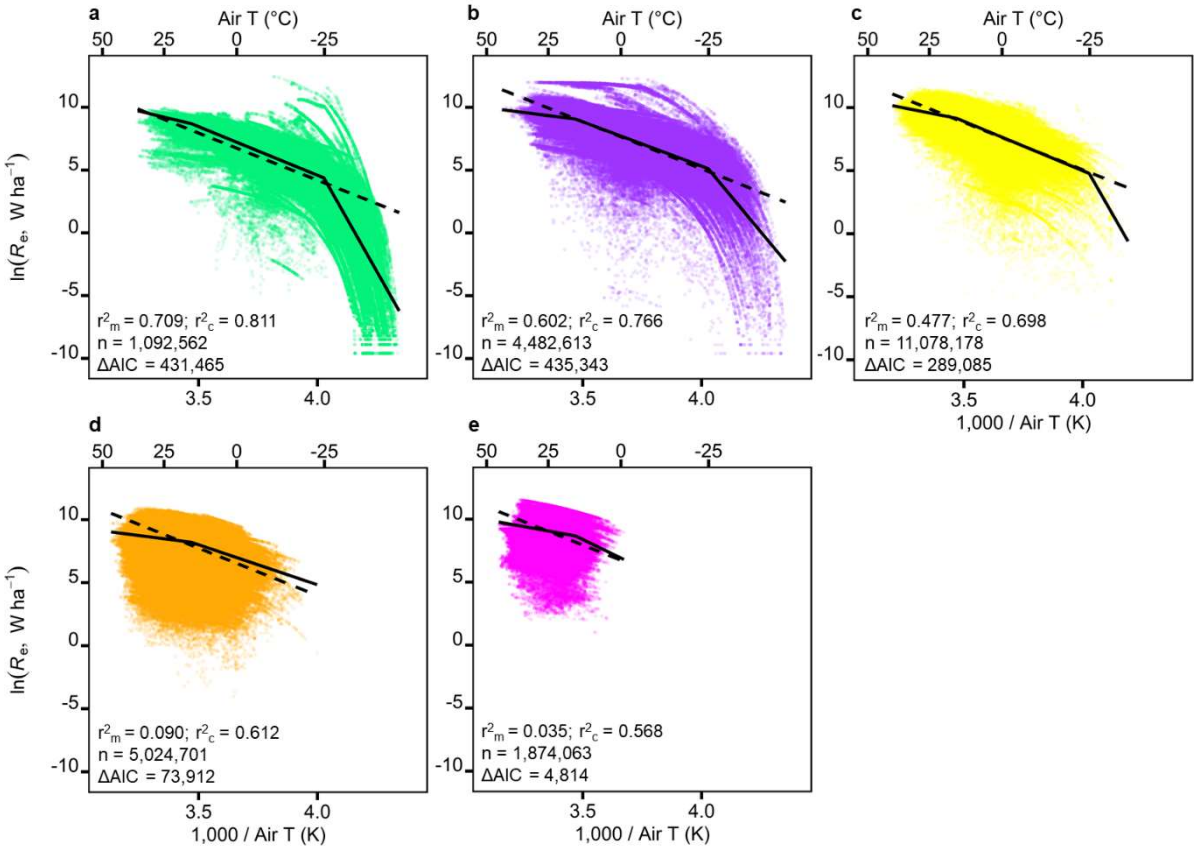

Figure 4. Temperature thresholds of ecosystem respiration (R_e) across five climates. Night-time half hourly ecosystem respiration measurements from the FLUXNET dataset (symbols), classified as a) tundra, b) boreal), c) temperate, d) mediterranean, and e) tropical, with symbol colours as in Figure 2. Solid lines show threshold model predictions for the fixed effects of temperature, and dashed lines show an activation energy of -7.5 K predicted by metabolic theory. ΔAICs indicate a greater goodness of fit of the threshold compared to linear model. Full details of the linear mixed effects models are presented in Supplementary Table 4.

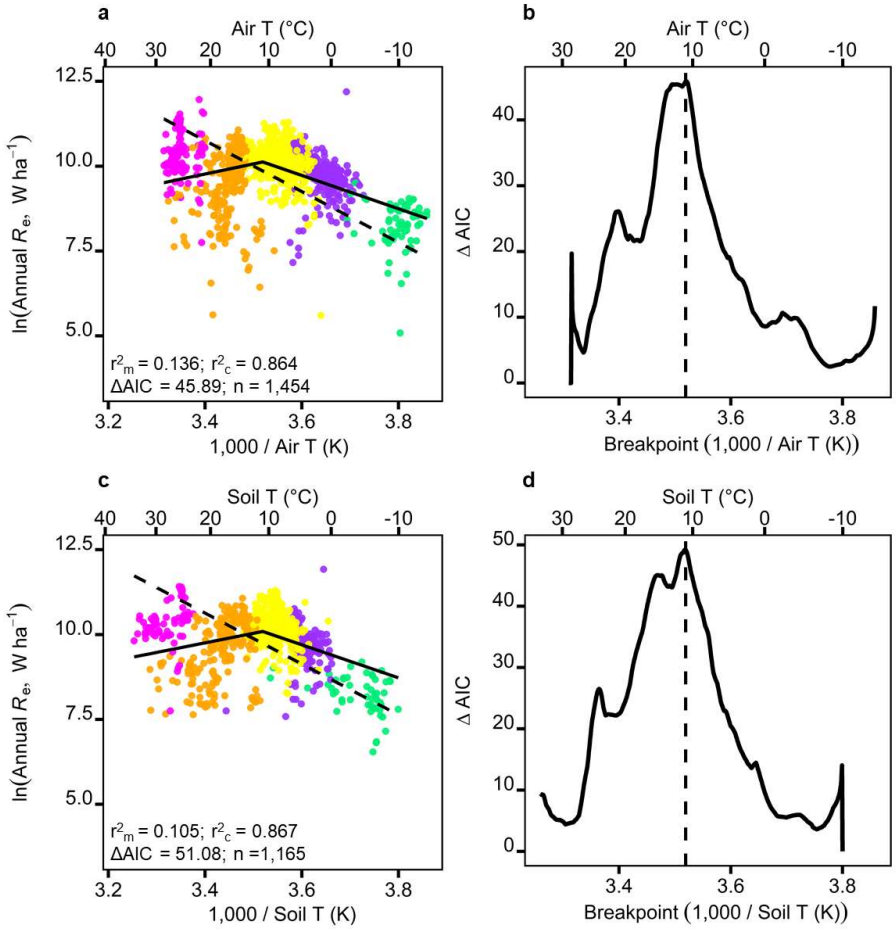

Figure 5. Long-term temperature thresholds of ecosystem respiration (R_e). Mean annual R_e and either a) air or c) soil temperature measurements (symbols), with symbol colours representing climate as in Figure 2. Plots show predictions from the threshold model (solid lines, for the fixed effects of temperature only). Both threshold models identified a single temperature breakpoint of 11.0 °C, with little support for a second temperature breakpoint (ΔAIC < 5 and p > 0.05). Dashed lines indicate an activation energy of -7.50 K as predicted by metabolic theory and ΔAICs are between the linear and threshold models. Full details of the threshold mixed effects models are presented in Supplementary Table 6.

Data availability

The dataset analysed during the current study is available on Dryad (https://doi.org/10.5061/dryad.70rxwdbwk).

Code availability

The R code used for analysis during the current study is available on Dryad (https://doi.org/10.5061/dryad.70rxwdbwk).

Acknowledgements

This work used eddy covariance data acquired and shared by the FLUXNET community and was supported by a Leverhulme Trust Research Project Grant (RPG-2017-071) and a Leverhulme Trust Research Leadership Award (RL-2019-012) to CV. AM was supported by BBSRC (BB/S019952/1) and the Leverhulme Trust (RPG-2019-170), PDB by the US Department of Energy Office of Science (7094866), DB by French Agence Nationale de la Recherche (ANR-10-LABX-25-01; ANR-11-LABX-0002-01), JD by the Ministry of Education, Youth and Sports of the Czech Republic (LM2015061), CG by a National Science Foundation Award (1655095), and AV by RFBR project 19-04-01234-a. We also thank Joanna Baker, George Butler and Ana Navarro Campoy for helpful discussions.

Author contributions

ASAJ and CV developed the methodology and led the writing of the manuscript. ASAJ and AM conduced the data analysis. JA, NA, DB, AB, PDB, CB, AC, JD, AG, BG, IG, CMG, HI, RJ, HK, VM, GM, LM, FEM, JEO, TS, CS, TT, GW, SW, WW, and AV contributed data. All authors contributed to manuscript revisions.

Competing interests

The authors declare no competing interests.